Desalination and Water Treatment
www.deswater.com
doi: 10.1080/19443994.2014.925833

55 (2015) 1445–1452
July

Taylor & Francis
Taylor & Francis Group

RSM and ANN modeling for electro-oxidation of simulated wastewater using CSTER

R. Saravanathamizhan[a,*], Kilaru Harsha Vardhan[a], D. Gnana Prakash[a], N. Balasubramanian[b]

[a]*Department of Chemical Engineering, SSN College of Engineering, Kalavakkam, Chennai 603 110, India, Tel. +91 44 27469700; emails: thamizhan79@rediffmail.com (R. Saravanathamizhan), kilaruh@ssn.edu.in (K. Harsha Vardhan), gnanaprakashd@ssn.edu.in (D. Gnana Prakash)*

[b]*Department of Chemical Engineering, A.C. Tech Campus, Anna University, Chennai 600 025, India, Tel. +91 44 22359190; email: nbsbala@annauniv.edu*

Received 11 September 2013; Accepted 14 May 2014

ABSTRACT

In this study, response surface methodology (RSM) and artificial neural network (ANN) were employed to develop prediction models for Acid Red 88 dye removal from synthetic wastewater using electro-oxidation. Experiments were carried out in a continuous stirred tank electrochemical reactor (CSTER) in once through approach using Ruthenium oxide-coated Titanium as anode and stainless steel sheet as cathode. The four operational parameters such as, effluent flow rate, initial dye concentration, current density, and pH, on chemical oxygen demand removal has been observed as a response. Experiments were conducted as per RSM of Box–Behnken design. The operating parameters were optimized and the models were developed using RSM and ANN. The ANN model of three hidden layers with two neuron networks, 4-2-2-2-1, matches well with the experimental observation.

Keywords: Acid Red 88; Artificial neural network; Chemical oxygen demand; Electro-oxidation; Response surface methodology

1. Introduction

The effluents discharged from textile industries are known to be strongly colored, have high chemical oxygen demand (COD), BOD, and fluctuating pH. Generally textile dye effluents can be treated by different methods such as biological methods, flocculation, adsorption on activated carbon, chemical oxidation methods, reverse osmosis, and advanced oxidation processes [1,2]. Conventional treatment process such as biological method, physical and chemical methods are found to be unsuccessful [3–5]. In recent years, researchers are focusing on advanced oxidation processes such as electrochemical technique [6], wet air oxidation [7], ozonation [8], photocatalytic oxidation [9], and ultrasonication [10] method for the degradation of organic pollutants. Among these advanced oxidation processes, the electrochemical treatment has been receiving greater attention in recent years due to its unique features, such as versatility, energy efficiency, automation, and cost effectiveness [11]. In recent years, there has been increasing interest in the use of electrochemical technique for the treatment of dye house effluent. The pollutants present in effluent,

*Corresponding author.

1944-3994/1944-3986 © 2014 Balaban Desalination Publications. All rights reserved.

are destroyed by an indirect anodic process via production of oxidants such as hypochloride, hydroxyl radicals. This technique has been successfully applied in the treatment of several industrial effluents [12,13].

Electrochemical process depends on various process parameters such as current density, effluent flow rate, supporting electrolyte concentration, pH, and initial effluent concentration. In conventional experimentation, experiments are conducted keeping all the variables constant except the parameter whose influence is being studied. But this approach does not determine the combined effect of all process parameters. Experimental design is an effective and efficient optimization strategy to overcome this drawback, which has gained wide application in chemical engineering optimization [14–16].

Researchers have applied response surface methodology (RSM) and artificial neural network (ANN) tools for the various processes. Ghosh et al. [17] studied copper removal from aqueous solution by chemically modified orange peel using central composite design for optimization and ANN for modeling. Marchitan et al. [18] compared RSM and ANN modeling for the reactive extraction of tartaric acid from aqueous solutions. Sinha et al. [19,20] applied RSM and ANN for the natural dye extraction from pomegranate rind and seeds of Bixa orellana. The author suggested that ANN has better prediction performance as compared to RSM. Geyikci et al. [21] studied RSM and ANN to develop models for lead removal from industrial sludge leachate using red mud. The author reported, ANN results were found to be more reliable than RSM. Bingol et al. [22] compared RSM and ANN for the biosorption of lead using black cumin. The authors reported that ANN model is much more accurate in prediction when compared to RSM of the central composite design.

RSM and ANN have been used for modeling various batch operation processes [23–25], but this paper is focused on continuous treatment of synthetic wastewater using electro-oxidation. ANN has become increasingly recommended for applications where the mechanistic description of the interdependence between variables is either unknown or the model is very complex, and requires lot of simplifications. One of the characteristics of modeling based on ANN is that it does not require the mathematical description of the phenomena involved in the process, and might therefore prove useful in simulating and up-scaling complex electrochemical systems. The objective of the study is to treat the Acid Red 88 dye effluent using Ruthenium oxide-coated Titanium as anode and stainless as a cathode in CSTER and develop a model using RSM and ANN techniques.

2. Materials and methods

All the chemicals used were of analytical grade (Ranbaxy, India). The synthetic wastewater of Acid Red 88 was prepared by dissolving the required amounts of dye in distilled water. The supporting electrolyte concentration (sodium chloride) was maintained constant at 750 mg l^{-1}. The pH of the initial dye solution is maintained by adding 0.1 N hydrochloric acid and 0.1 N sodium hydroxide solutions, and is monitored using a digital pH meter (Eclico, Model Li 120). The initial dye concentrations (50, 75, and 100 mg l^{-1}) are estimated by a standard estimation procedure [26] in terms of chemical oxygen demand (300, 475, and 650 mg l^{-1}). Color of the dye is measured using UV–vis spectrophotometer as absorbance and calculated in terms of concentration using the calibration chart (concentration of the dye vs. absorbance). After electro-oxidation, the absorbance is measured and the corresponding concentration is calculated using the calibration chart. Then the percentage color removal is calculated as:

$$\text{Color removal}\,(\%) = \frac{\text{initial dye concentration} - \text{final dye concentration}}{\text{initial dye concentration}} \times 100 \tag{1}$$

2.1. Experimental setup

The experimental setup of the once through mode of operation is schematically represented in Fig. 1. The continuous stirred tank electrochemical reactor (CSTER), consists of a stainless steel sheet cathode and Ruthenium oxide-coated Titanium as anode, measuring $6.5 \times 5\ \text{cm}^2$. The reactor volume is 300 ml and electrodes used were fixed inside the reactor with a 1 cm space between them. The flow rates are adjusted by a peristaltic pump. The flow rates are varied (25, 50, and 75 ml min^{-1}) to get their corresponding residence times (12, 6, and 4 min).

2.2. Treatment in once through mode

The electrochemical cell has an inlet and outlet at the bottom and top, respectively. The electrodes were connected to a 5 A, 30 V DC-regulated power supply (HIL model 3161). The other components of the setup such as feed reservoir having a capacity of 1 l and a peristaltic pump are connected using silicone rubber tubes. The reservoir was filled with necessary quantity of synthetic effluent for various initial concentrations. The supporting electrolyte (sodium chloride) concentration of 750 mg l^{-1} is maintained constant for all studies. The flow rate required through the reactor was established by the peristaltic pump. Various operating

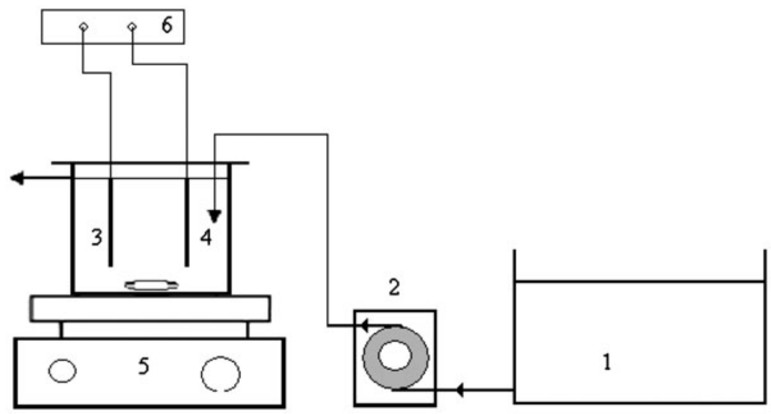

Fig. 1. Schematic representation of CSTER; (1) effluent storage tank; (2) peristaltic pump; (3) anode; (4) cathode; (5) magnetic stirrer; and (6) DC power supply.

parameters such as effluent flow rate (25–100 ml min^{-1}), initial dye concentration (50–100 mg l^{-1}), current density (2–10 mA cm^{-2}), and initial solution pH (4–10) were selected for the percentage COD removal estimation. Every experimental run samples were collected from the reactor, at a steady-state condition for the determination of color and COD removal.

2.3. Box–Behnken design

In the present work, the Box–Behnken experimental design has been chosen to find the relation between the output response and input variables. Box–Behnken design is a rotatable second-order design based on three level incomplete factorial designs. For the present investigation, Table 1 shows the level of each variable. Table 2 shows experimental runs for a three-level, four-factor Box–Behnken design with three center points designed using MINITAB 14 (PA, USA). The analysis was focused on the COD reduction which is influenced by independent variables, i.e. effluent flow rate (*A*), initial dye concentration (*B*), current density (*C*), and pH (*D*).

Table 1
Range of variables chosen for electro-oxidation of Acid Red 88 using Box–Behnken design

Factor	Variables	Unit	Range of actual and coded variables		
			−1	0	+1
A	Flow rate	ml min^{-1}	25	50	75
B	Initial dye concentration	mg l^{-1}	50	75	100
C	Current density	mA cm^{-2}	2	6	10
D	pH	–	4	7	10

3. Results and discussion

3.1. Single-pass flow

Pollutant removal of the single-pass flow reactor was studied by varying current density (2–10 mA cm^{-2}) and flow rate (25–100 ml min^{-1}). Fig. 2 shows that an increase in current density improves the pollutant removal. In other words, operation of the cell at a higher current density increases the COD removal. This is due to the fact that the rate of generation of hypochlorite ion increases with an increase in current density, which eventually increases the pollutant degradation. It is also observed from Fig. 2, the amount of COD removal in the reactor is less due to lower residence time for the higher flow rate. Based on the single-pass flow experiments, the level of the experimental parameters has been selected for the RSM.

3.2. RSM modeling

The mathematical relationship of COD removal with operating variables such as flow rate (*A*), initial dye concentration (*B*), current density (*C*), and initial solution pH (*D*) can be given as uncoded form:

$$\begin{aligned}\%\mathrm{COD} = {} & 55.799 + 1.016A - 1.347B + 3.419C - 2.444D \\ & - 0.008A^2 + 0.008B^2 + 0.020C^2 + 0.962D^2 \\ & + 0.003AB + 0.006AC - 0.126AD - 0.0116BC \\ & - 0.02BD + 0.072CD \end{aligned} \tag{2}$$

Table 2
Actual design of experiments and Color, COD removal for electro-oxidation

Exp. run	*A* ml min^{-1}	*B* mg l^{-1}	*C* mA cm^{-2}	*D* –	*a*	*b*	*c*	*d*	Color removal (%)	COD removal (%)
	(Uncoded unit)				Coded unit					
1	25	50	6	7	−1	−1	0	0	61.15	55.00
2	25	100	6	7	−1	1	0	0	45.05	38.62
3	25	75	2	7	−1	0	−1	0	37.12	29.30
4	25	75	10	7	−1	0	1	0	57.58	55.82
5	25	75	6	4	−1	0	0	−1	45.21	29.88
6	25	75	6	10	−1	0	0	1	85.20	75.49
7	50	75	2	4	0	0	−1	−1	28.05	21.24
8	50	75	10	4	0	0	1	−1	58.75	48.87
9	50	75	2	10	0	0	−1	1	52.99	43.59
10	50	75	10	10	0	0	1	1	87.53	74.77
11	50	50	6	4	0	−1	0	−1	55.00	51.00
12	50	100	6	4	0	1	0	−1	46.00	44.91
13	50	50	6	10	0	−1	0	1	75.53	57.59
14	50	100	6	10	0	1	0	1	59.47	55.51
15	50	50	2	7	0	−1	−1	0	30.00	28.57
16	50	100	2	7	0	1	−1	0	24.37	21.54
17	50	50	10	7	0	−1	1	0	60.00	58.57
18	50	100	10	7	0	1	1	0	55.00	45.89
19	50	75	6	7	0	0	0	0	45.23	37.50
20	50	75	6	7	0	0	0	0	45.23	37.50
21	50	75	6	7	0	0	0	0	45.23	37.5
22	75	50	6	7	1	−1	0	0	35.25	34.00
23	75	100	6	7	1	1	0	0	32.00	25.00
24	75	75	2	7	1	0	−1	0	15.08	14.90
25	75	75	10	7	1	0	1	0	47.50	44.60
26	75	75	6	4	1	0	0	−1	35.21	15.93
27	75	75	6	10	1	0	0	1	32.85	25.55

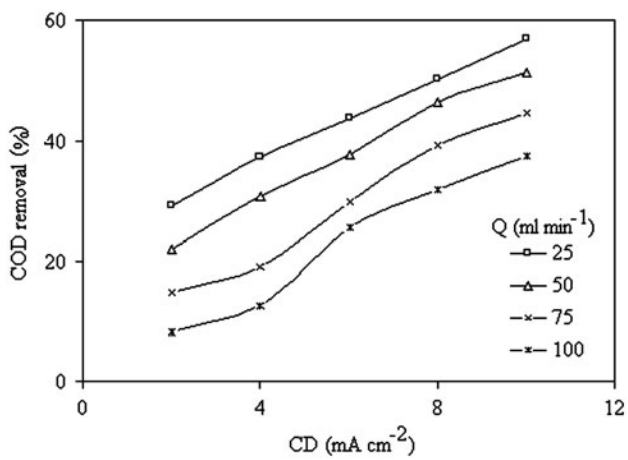

Fig. 2. Effect of effluent flow rate on percentage COD removal.

The prediction of COD removal using the above equation has been compared with experimental values given in Table 2 (Fig. 3). It is observed from Fig. 3, the model predictions match satisfactorily with the experimental values. The parameters according to Eq. (2), have been optimized for the maximum percentage COD removal and the optimized values for 95% COD removal is 25 ml min^{-1} of effluent flow rate, 50 mg l^{-1} of initial dye concentration, 10 mA cm^{-2} of current density, and pH of the dye solution is 10.

The RSM has been applied to electro-oxidation of Acid Red 88 dye effluent in CSTER and the results are presented in three-dimensional surface plots. The interaction between effluent flow rate and initial effluent concentration is given in Fig. 4. It is observed from Fig. 4, that the percentage COD removal increases with decrease in initial dye concentration and flow rate of effluent. This is evident that the generation of organic intermediates is more stable for the high-initial dye concentration and thus decreases the COD removal.

The combined effects of initial dye concentration and current density on percentage COD removal is shown in Fig. 5. It is observed from Fig. 5 that the

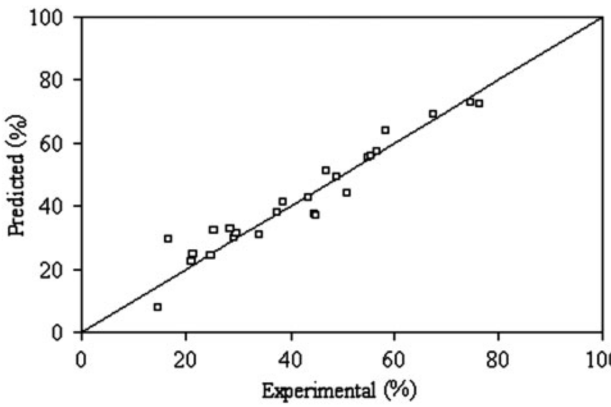

Fig. 3. Comparison of model prediction with experimental observations on percentage COD removal.

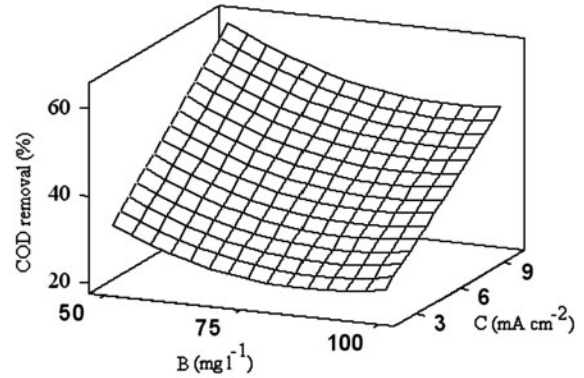

Fig. 5. Response surface plot of initial dye concentration and current density on percentage COD removal. Flow rate: 25 ml min^{-1}; pH 7.0.

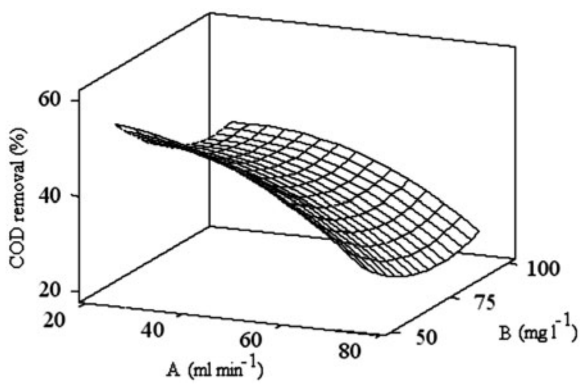

Fig. 4. Response surface plot of flow rate and initial dye concentration on percentage COD removal. Current density: 6 mA cm^{-2}; pH 7.0.

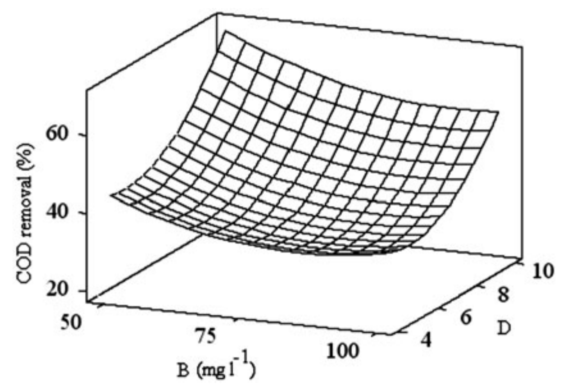

Fig. 6. Response surface plot of initial dye concentration and pH on percentage COD removal. Flow rate: 25 ml min^{-1}; current density: 6 mA cm^{-2}.

percentage COD removal increases with increase in current density and decreases with increase in initial dye concentration. Increasing current density increases the hypochlorite formation which results in increase in percentage COD removal.

The analysis on combined effect of initial dye concentration and pH on percentage COD removal is given in the three-dimensional surface plots. It is ascertained from Fig. 6 that COD removal increases with increase in pH and decreases with increase in initial dye concentration. The reaction is favorable in basic due to increased formation OCl^- ion. At high-initial dye concentration, the generation of organic intermediates is more stable compared to low initial dye concentration which results in decrease in percentage COD removal. The individual plots of various process parameters on percentage COD removal are shown in Fig. 7. It is observed from this figure that the percentage COD removal decreases with increase in effluent flow rate, initial dye concentration, and COD removal increases with increase in current density and initial pH of the effluent.

Analysis of variance (ANOVA) is applied to determine the significant effects of process variables on output response and the results are shown in Table 3. The *F* values comparison has been performed at 5% level. It is noticed from Table 3 that the *F* values for percentage COD removal is higher which indicates that the variation in the responses can be explained by the present model. Further, the associated *P* values are used to estimate whether the *F* values are large enough to indicate statistical significance or not. It is noticed that, the *F* value of 10.79 (Table 3) is higher than the standard $F_{0.05(14,12)}$ value of 2.60, which shows that percentage COD removal is significant. In general, *P* values less than 0.01 are considered to be significant in statistical model. It is observed from Table 3, the *P* values obtained using Eq. (1) is 0.000,

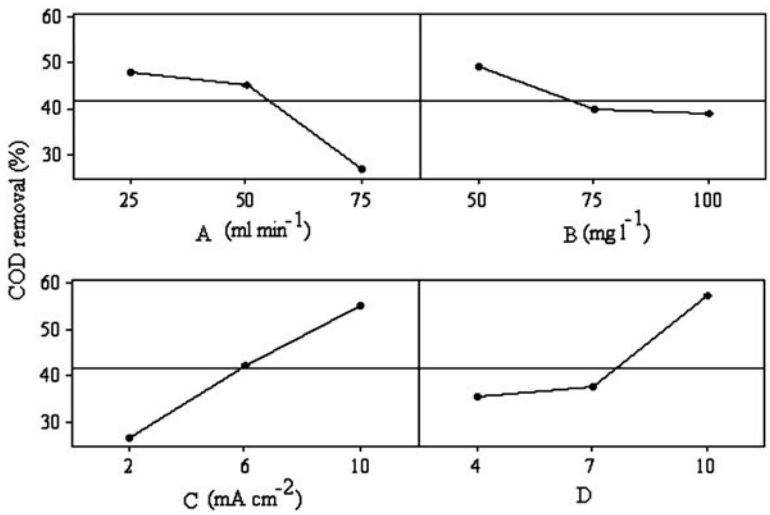

Fig. 7. Individual plot for percentage COD removal.

Table 3
ANOVA for percentage COD removal using RSM

Source	Degree of freedom	Sum of square	Mean square	*F*	*P*
Regression	14	6784.70	484.621	10.79	0.000
Linear	4	5497.63	92.737	2.07	0.149
Square	4	894.29	223.572	4.98	0.013
Interaction	6	392.78	65.463	1.46	0.272
Residual error	12	538.89	44.907		
Lack-of-fit	10	538.89	53.889		
Pure error	2	0.00	0.000		
Total	26	7323.58			

Note: $R^2 = 0.925$; $R^2_{adj} = 0.841$.

show that the present model is significant. The present model equations are further checked by regression coefficients (R^2 and R^2_{adj}) and the values of R^2 and R^2_{adj} are 0.926 and 0.841, which indicate that the model is highly significant.

3.3. ANN modeling

Several models for ANN exist. The back propagation neural network (BPNN) is most widely used in chemical engineering. In the present study, BPNN, *Trainlm*, and *Tannsig* functions are selected as a network, training function, and transfer function, respectively. Generally neural networks consist of input layer, hidden layers, and output layer. Different hidden layers and neurons are selected for training and prediction of output response of the process. In the present work for the development of ANN Model, 120 different combinations of experimental runs were selected by changing one parameter at a time keeping all the other three parameters constant. Out of which 80 were randomly selected for the training, 15 were used for the validation, and 25 were used for the simulation. The input variables are effluent flow rate, initial dye concentration, current density, and pH. Percentage COD removal is the output layer for the ANN model. Training is started from one hidden layer to three hidden layers. The number of neurons that varied for the present model is shown in Table 4. A feed-forward ANN model is designed in back-propagation training algorithm using the neural network toolbox of MATLAB 7. All the outputs are linearly normalized using Eq. (3) before entering in to ANN,

$$A_i = \frac{(X_i - X_{\min})}{(X_{\max} - X_{\min})}(r_{\max} - r_{\min}) + r_{\min} \tag{3}$$

Table 4
Number of hidden layer, number of neurons selected for the present ANN model, and their RMSE and MAPE

No. of hidden layer	No. of neurons	RMSE	MAPE (%)
1	1	8.16	15.73
	2	8.16	15.73
	3	6.05	13.88
	4	6.31	16.57
	5	5.11	12.59
	10	31.70	43.74
2	1	8.14	15.73
	2	7.98	20.44
	3	5.77	14.38
	4	4.92	11.68
	5	4.92	11.68
	10	4.93	11.69
3	1	8.13	15.73
	2	4.16	8.88
	3	5.05	12.40
	4	5.05	12.60
	5	4.93	11.69
	10	4.93	11.69

where X_i is input or output of the network, A_i is the normalized value of X_i, $X_{\min}$ and $X_{\max}$ are extreme values of X_i, and $r_{\min}$ and $r_{\max}$ define the limits of the range where X_i is scaled. In the present work, input and output data were normalized between −1 to 1; and 0–0.9, respectively. After modeling, results are converted to original state. The hidden layer and neurons are selected based on following equations and the values are tabulated in Table 4.
Root-mean-square-error (RMSE)

$$\mathrm{RMSE} = \sqrt{\frac{\sum_{i=1}^{N} (E_{p,i} - E_{a,i})^2}{N}} \tag{4}$$

Maximum average percentage error (MAPE)

$$\mathrm{MAPE} = \frac{1}{N}\sum_{i=1}^{N} \frac{|E_{p,i} - E_{a,i}|}{E_{a,i}} \times 100 \tag{5}$$

where E_p and E_a are the predicted and actual values, respectively. N is the number of data-set. It is observed form Table 4, that three hidden layer with two neurons show less RMSE and MAPE values. The predicted value using ANN model compared with experimental observation is shown in Fig. 8. It is observed from the figure, the ANN model with three hidden layers and two neuron networks, 4-2-2-2-1, satisfactorily matches with the experimental observations.

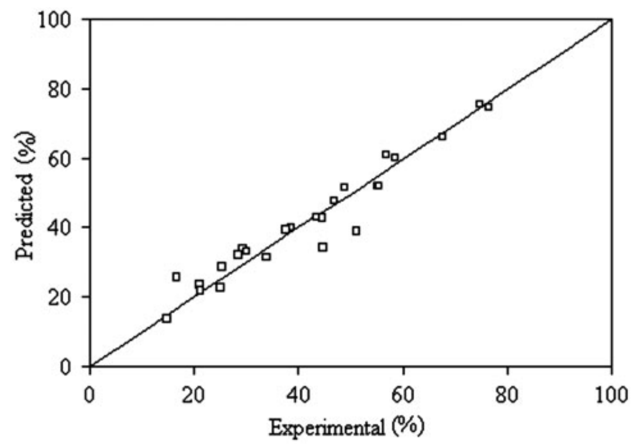

Fig. 8. Comparison of ANN model prediction with experimental observations on percentage COD removal.

4. Conclusions

In the present study, electro-oxidation of Acid Red 88 dye house effluent was studied using Ruthenium oxide-coated electrode in a CSTER. An effort has been made to model the electro-oxidation process using RSM and ANN. Response surface plot provides a good way of visualizing the parameter's interaction and the resulting model with $R^2 = 0.925$ shows that the model is in good agreement with the experimental COD removal for the electro oxidation of dye effluent. The ANN model with network structure 4-2-2-2-1, satisfactorily matches with the experimental observations.

References

[1] C. Özdemir, M.K. Öden, S. Şahinkaya, E. Kalipçi, Color removal from synthetic textile wastewater by sono-fenton process, Clean—Soil, Air, Water 39 (2011) 60–67.
[2] Y.M. Slokar, A. Majcen Le Marechal, Methods of decoloration of textile wastewaters, Dyes Pigm. 37 (1998) 335–356.
[3] C.I. Pearce, J.R. Lloyd, J.T. Guthrie, The removal of colour from textile wastewater using whole bacterial cells: A review, Dyes Pigm. 58 (2003) 179–196.
[4] M. Liu, Z. Lü, Z. Chen, S. Yu, C. Gao, Comparison of reverse osmosis and nanofiltration membranes in the treatment of biologically treated textile effluent for water reuse, Desalination 281 (2011) 372–378.
[5] A. Baban, A. Yediler, D. Lienert, N. Kemerdere, A. Kettrup, Ozonation of high strength segregated effluents from a woollen textile dyeing and finishing plant, Dyes Pigm. 58 (2003) 93–98.
[6] A. Fernandes, A. Morao, M. Magrinho, A. Lopes, I. Goncalves, Electrochemical degradation of C. I. acid orange 7, Dyes Pigm. 61 (2004) 287–296.
[7] B. Kayan, B. Gözmen, M. Demirel, A.M. Gizir, Degradation of acid red 97 dye in aqueous medium using wet oxidation and electro-Fenton techniques, J. Hazard. Mater. 177 (2010) 95–102.

[8] P. Asaithambi, M. Susree, R. Saravanathamizhan, M. Matheswaran, Ozone assisted electrocoagulation for the treatment of distillery effluent, Desalination 297 (2012) 1–7.
[9] M.N. Vineetha, M. Matheswaran, K.N. Sheeba, Photocatalytic colour and COD removal in the distillery effluent by solar radiation, Sol. Energy 91 (2013) 368–373.
[10] S. Anusha, P. Asaithambi, M. Susree, M. Matheswaran, Sonoelectrochemical oxidation for decolorization of reactive red 195, Ultrason. Sonochem. 19 (2012) 803–811.
[11] F.C. Walsh, Electro chemical technology for environmental treatment and clean energy conversion, Pure Appl. Chem. 73 (2001) 1819–1837.
[12] A.G. Vlyssides, D. Papaioannou, M. Loizidoy, P.K. Karlis, A.A. Zorpas, Testing an electrochemical method for treatment of textile dye wastewater, Waste Manage. 20 (2000) 569–574.
[13] S. Mahesh, B. Prasad, I.D. Mall, I.M. Mishra, Electrochemical degradation of pulp and paper mill wastewater. Part 1. COD and color removal, Ind. Eng. Chem. Res. 45 (2006) 2830–2839.
[14] B.K. Körbahti, Response surface optimization of electrochemical treatment of textile dye wastewater, J. Hazard. Mater. 145 (2007) 277–286.
[15] B.K. Körbahti, N. Aktaş, A. Tanyolaç, Optimization of electrochemical treatment of industrial paint wastewater with response surface methodology, J. Hazard. Mater. 148 (2007) 83–90.
[16] A. Aleboyeh, N. Daneshvar, M.B. Kasiri, Optimization of C.I. acid red 14 azo dye removal by electrocoagulation batch process with response surface methodology, Chem. Eng. Process. 47 (2008) 827–832.
[17] D. Ghosh, R. Saha, A. Ghosh, R. Nandi, B. Saha, A review on toxic cadmium biosorption from contaminated wastewater, Desalin. Water Treat. 51 (2013) 1–8.
[18] N. Marchitan, C. Cojocaru, A. Mereuta, G. Duca, I. Cretescu, M. Gonta, Modeling and optimization of tartaric acid reactive extraction from aqueous solutions: A comparison between response surface methodology and artificial neural network, Sep. Purif. Technol. 75 (2010) 273–285.
[19] K. Sinha, P.D. Saha, S. Datta, Response surface optimization and artificial neural network modeling of microwave assisted natural dye extraction from pomegranate rind, Ind. Crops Prod. 37 (2012) 408–414.
[20] K. Sinha, S. Chowdhury, P.D. Saha, S. Datta, Modeling of microwave-assisted extraction of natural dye from seeds of bixa orellana (annatto) using response surface methodology (RSM) and artificial neural network (ANN), Ind. Crops Prod. 41 (2013) 165–171.
[21] F. Geyikçi, E. Kılıç, S. Çoruh, S. Elevli, Modelling of lead adsorption from industrial sludge leachate on red mud by using RSM and ANN, Chem. Eng. J. 183 (2012) 53–59.
[22] D. Bingöl, M. Hercan, S. Elevli, E. Kılıç, Comparison of the results of response surface methodology and artificial neural network for the biosorption of lead using black cumin, Bioresour. Technol. 112 (2012) 111–115.
[23] A. Arul Murugan, R. Thilakavathi, N. Balasubramanian, C. Srinivasa Kannan, G. Madhavi, Electrocoagulation of textile effluent: RSM and ANN modeling, Inter. J. Chem. React. Eng. 7 (2009) 1–14.
[24] S. Aber, A.R. Amani-Ghadim, V. Mirzajani, Removal of Cr(VI) from polluted solutions by electrocoagulation: Modeling of experimental results using artificial neural network, J. Hazard. Mater. 171 (2009) 484–490.
[25] N. Daneshvar, A.R. Khataee, N. Djafarzadeh, The use of artificial neural networks (ANN) for modeling of decolorization of textile dye solution containing C. I. basic yellow 28 by electrocoagulation process, J. Hazard. Mater. 137 (2006) 1788–1795.
[26] Standard Methods for Examination of Water and Wastewater, 17th ed., American Public Health Association, Washington, DC, 1989.